

# Interaction of Hematoporphyrin with Lipid Membranes

Michał Stępniewski,<sup>†,‡</sup> Mariusz Kepczynski,<sup>\*,†</sup> Dorota Jamróz,<sup>†</sup> Maria Nowakowska,<sup>†</sup> Sami Rissanen,<sup>§</sup> Ilpo Vattulainen,<sup>§,||</sup> and Tomasz Róż<sup>\*,§</sup>

<sup>†</sup>Faculty of Chemistry, Jagiellonian University, Ingardena 3, 30-060 Kraków, Poland

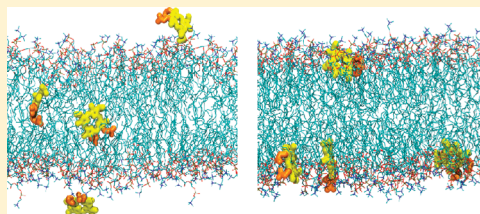
<sup>‡</sup>Centre for Drug Research, Faculty of Pharmacy, University of Helsinki, Helsinki, Finland

<sup>§</sup>Department of Physics, Tampere University of Technology, PO Box 692, FI-33101 Tampere, Finland

<sup>||</sup>MEMPHYS-Center for Biomembrane Physics, University of Southern Denmark, Odense, Denmark

## Supporting Information

**ABSTRACT:** Natural or synthetic porphyrins are being used as photosensitizers in photodiagnosis (PD) and photodynamic therapy (PDT) of malignancies and some other diseases. Understanding the interactions between porphyrins and cell membranes is therefore important to rationalize the uptake of photosensitizers and their passive transport through cell membranes. In this study, we consider the properties of hematoporphyrin (Hp), a well-known photosensitizer for PD and PDT, in the presence of a 1-palmitoyl-2-oleoyl-*sn*-glycero-3-phosphocholine (POPC) bilayer that we use as a model system for protein-free cell membranes. For this purpose, we employed 200 ns atomic-scale molecular dynamics (MD) simulations for five systems containing the neutral ( $\text{Hp}^0$ ) or the dianionic form ( $\text{Hp}^{2-}$ ) of Hp and the POPC bilayer. MD simulations allowed one to estimate the position, orientation, and dynamics of Hp molecules inside the membrane. The dye molecules were found to reside in the phospholipid headgroup area close to the carbonyl groups of the POPC acyl chains. Their orientations were dependent on the protonation state of two propionic groups.  $\text{Hp}^{2-}$  was found to have a lower affinity to enter the membrane than the neutral form. The dianions, being in the aqueous phase, formed stable dimers with a strictly determined geometry. Our results fully supported the experimental data and provide a more detailed molecular-level description of the interactions of photosensitizers with lipid membranes.



## 1. INTRODUCTION

Porphyrins with various side groups attached to a porphin ring have been used as photosensitizers in cancer photodiagnosis (PD) and photodynamic therapy (PDT).<sup>1,2</sup> PD and PDT are promising modalities shown to be effective in the early detection and treatment of several types of malignant and nonmalignant diseases. Both of these methods involve administration of a photosensitizing agent, which is preferentially taken up and retained by diseased tissue. Upon activation with light of a specific wavelength, that agent can fluoresce and generate the reactive oxygen species. Fluorescence is used as a very sensitive indicator in PD, while a sequence of photochemical and photobiological processes, initiated by the reactive oxygen species and causing photodamage of tumor tissues, is known as PDT.

Hematoporphyrin (Hp) occupies a particular position among the photosensitizers for PD and PDT.<sup>3</sup> It is being used as a photosensitizer in clinical cancer research, because it is readily absorbed by cancerous tissue and fluoresces effectively after excitation.<sup>4</sup> In 1960, Lipson and Schwartz observed that injection of Hp led to fluorescence of neoplastic lesions visualized during surgery.<sup>2</sup> In further studies to enhance dye accumulation in the tumor, Lipson et al.<sup>5</sup> synthesized a hematoporphyrin derivative (HpD), which is a complex mixture of monomeric and aggregated porphyrins used in the photodynamic therapy of tumors. Preclinical studies performed

by Dougherty et al.<sup>1,6</sup> showed that HpD caused very efficient tumor necrosis. A purified component of this mixture is known as dihematoporphyrin ether commercially available as Photofrin. It is the first photosensitizer approved by the Food and Drug Administration for specific clinical applications.<sup>7</sup>

Interactions between Hp and cell membranes are important due to their crucial role in the processes of the photosensitizer uptake and its passive transport through cell membranes.<sup>8</sup> Jori et al.<sup>3</sup> studied the pharmacokinetic profile of the hematoporphyrin encapsulated into small unilamellar dipalmitoylphosphatidylcholine (DPPC) vesicles in comparison to dye dissolved in phosphate buffer saline (PBS). The *in vivo* study in MS-2 fibrosarcoma-bearing mice has shown that, despite a slow rate of dye accumulation in the tumor, its maximum concentration was higher than that with the PBS formulation. In spite of a large number of papers concerning partitioning of Hp into lipid membranes,<sup>9–11</sup> only some qualitative estimation of Hp location inside the bilayer can be found in the literature. Using fluorescence methods, Ricchelli and Gobbo have demonstrated that Hp embedded in a lipid bilayer interacts with very polar, solvent-accessible regions of the membrane.<sup>12</sup>

Received: January 27, 2012

Revised: April 1, 2012

Published: April 7, 2012

Generally, the depth-localization and orientation of porphyrins inside a cell membrane are relatively poorly recognized in the literature. We have found only one study on the depth-localization of porphyrins in the bilayer. The localization of the series of protoporphyrins with varying lengths of alkyl carboxylate side groups was studied using the fluorescence quenching analysis (FQA) method.<sup>13</sup> It was found that the distance of the effective center of the protoporphyrin fluorophore from the center of the bilayer changes from ~1.9 nm (the fluorophore is practically close to the water interface) to ~0.7 nm upon elongation of alkyl carboxylate groups. It seems that further studies are necessary to obtain a deep insight into the behavior of Hp in lipid membranes.

Computer simulations provide a complementary view to experiments, revealing a level of detail that is often very difficult or even impossible to achieve experimentally.<sup>14</sup> Application of molecular dynamics (MD) simulations to study interactions of small molecules with lipid bilayers has previously been reviewed by MacCallum and Tielemans<sup>14</sup> and Xiang and Anderson.<sup>15</sup> MD simulations can be useful in studies of a number of issues related to those interactions, such as preferential localization, orientation, partitioning into membranes (especially important in liposomal drug transport), permeation through membranes, and effects on lipid bilayer properties. In a previous paper, we used MD simulations to study the position and orientation of 2,6-bis(decyloxy)naphthalene inside a lipid bilayer and the possibility of a translocation (flip-flop) of this compound from one monolayer to the other. Curdova et al. used MD simulations in studies of free pyrene inside gel- and fluid-like phospholipid membranes.<sup>16</sup> They found that pyrene molecules prefer to be located within the hydrophobic acyl chain region, close to the glycerol group of lipid molecules. Their orientation depends though on the phase of the membrane. In the fluid phase, pyrene favors the orientation parallel to the membrane normal, while in the gel phase the orientation is affected by the tilt of the lipid acyl chains.

In this article, we present the results of atom-scale MD simulations on the interactions of porphyrin with a model membrane. To our knowledge, no computational study of such interactions has been previously published. We consider the behavior of Hp in the interior and at the surface of a 1-palmitoyl-2-oleoyl-sn-glycero-3-phosphocholine (POPC) bilayer. First, the depth-localization of the porphyrin and its orientation with respect to lipid molecules are determined. Next, we consider dynamic behavior, and in particular lateral and rotational motions of Hp molecules inside a membrane. Further, we focus on the possibility of formation of hydrogen bonds and charge pairs between porphyrin and lipid molecules, and between porphyrin and water molecules. Finally, the formation of Hp dimers and their geometry in the aqueous phase is also discussed.

## 2. METHODS

**2.1. Model Systems.** We performed atomistic molecular dynamics (MD) simulations of lipid bilayers composed of 128 POPC (1-palmitoyl-2-oleoyl-sn-glycero-3-phosphocholine) and 4 hematoporphyrin (Hp) molecules (Figure 1). For POPC, we used a previously equilibrated bilayer.<sup>17</sup> All membranes were fully hydrated with approximately 4500 water molecules. As Hp is able to dissociate in aqueous solution depending on the pH of the environment, we simulated five different systems: two systems containing the neutral form of Hp (referred to as  $\text{Hp}^0$ ) and three systems with the dianionic form of porphyrin

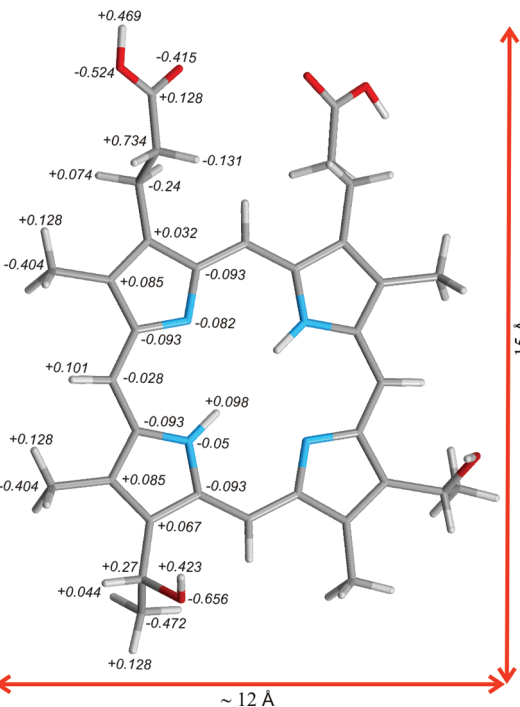
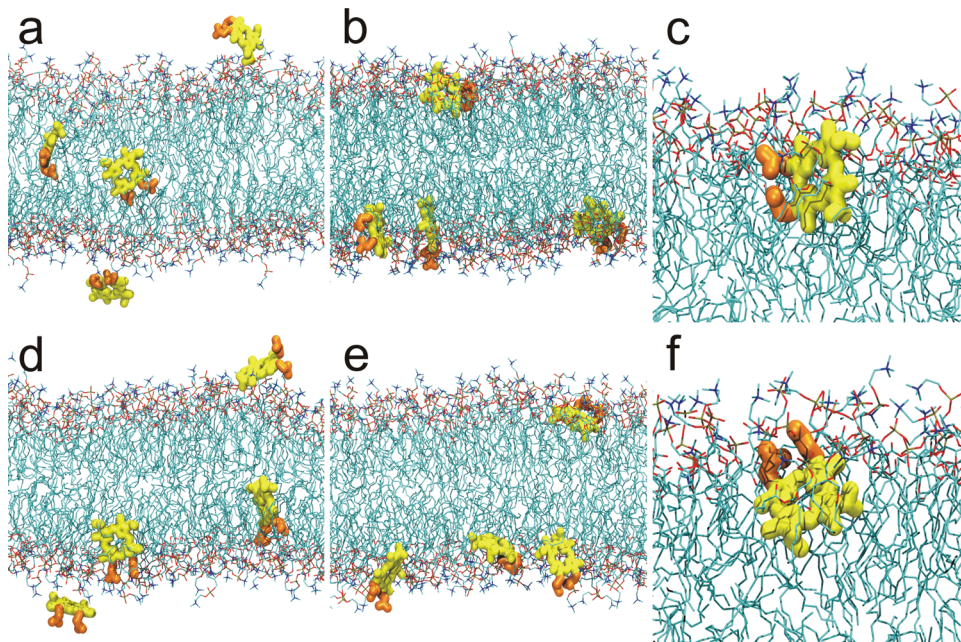


Figure 1. Structure of hematoporphyrin (Hp) with partial charges marked.

dissociated at the carboxylic groups (referred to as  $\text{Hp}^{2-}$ ). Each of the five different systems contained four Hp molecules that were initially placed at different positions with different orientations inside a membrane or in the aqueous phase (Figure 2a and c). In each system, two molecules were set with the porphyrin rings close to the center of the membrane and in parallel to the membrane normal. The two remaining molecules were placed in the aqueous phase with the ring planes almost parallel to the membrane surface.

Lipid and Hp molecules were parametrized using the all-atom OPLS force field.<sup>18</sup> Partial charges for the POPC molecule are part of the OPLS parametrization for standard units and sugars. However, since the partial charges on the PC headgroups were not originally included in the OPLS set, they were taken from Takaoka et al.<sup>19</sup> This set of charges was derived in compliance with the OPLS methodology. The chemical structure of the HP molecule is shown in Figure 1. Partial charges for the HP molecule were calculated according to the RESP methodology.<sup>20,21</sup> Since the RESP derived charges are known to suffer from conformational dependence,<sup>22</sup> three conformations of the HP molecule, differing in the orientation of the propionate moieties with respect to the porphine ring plane, were taken into account. The conformers were energy minimized at the HF/6-31G\* level of theory, and for each resulting geometry, the molecular electrostatic potential (MEP) grid was computed according to the Merz–Kollman scheme.<sup>23,24</sup> The energy and MEP calculations were performed using the Gaussian 03 program.<sup>25</sup> A multiconfiguration charge fitting was performed with the RESP program by imposing constraints due to local symmetry or chemical equivalence of atoms. The resulting partial charges are shown in Figure 1. For water, we employed the TIP3P model, which is compatible with the OPLS parametrization.<sup>26</sup> The system setup used in this study for POPC and water molecules is identical to the one



**Figure 2.** Snapshots of the configurations at  $t = 0$  and 200 ns for  $\text{Hp}^0$  (a, b) and  $\text{Hp}^{2-}$  (d, e). (c) Enlargement of one  $\text{Hp}^0$  molecule shown in panel b. (f) Enlargement of one  $\text{Hp}^{2-}$  molecule shown in panel e. The four  $\text{Hp}$  molecules are shown in yellow as a licorice representation for the porphyrin ring, and in orange for the propionic acid groups. POPC lipids are shown as sticks and colored as follows: blue, nitrogen; brown, phosphate; red, oxygen; and cyan, hydrocarbon chains. For clarity, water molecules are not shown.

used in our previous simulation of lipid bilayers with OPLS-AA parametrization.<sup>17,27</sup>

Periodic boundary conditions with the usual minimum image convention were used in all three directions. The LINCS algorithm was used to preserve hydrogen covalent bond lengths.<sup>28</sup> The time step was set to 2 fs, and the simulations were carried out at constant pressure (1 bar) and temperature (310 K). The temperature and pressure were controlled using the Parrinello–Ramman and Nose–Hoover method, respectively.<sup>29,30</sup> The temperatures of the solute and the solvent were controlled independently. For pressure, we used a semi-isotropic control. The Lennard-Jones interactions were cut off at 1.0 nm, and for the electrostatic interactions, we employed the particle mesh Ewald method<sup>31</sup> with a real space cutoff of 1.0 nm,  $\beta$ -spline interpolation (order of 6), and direct sum tolerance of  $10^{-6}$ . The simulation protocol used in this study has been successfully applied in various molecular dynamics simulation studies of lipid bilayers.<sup>32,33</sup>

Finally, prior to actual MD simulations that were performed using the GROMACS 4.0.3 software package,<sup>34</sup> the steepest-descent algorithm was used to minimize the energy of the initial structure. MD simulations were carried out over 200 ns in each of the modeled systems.

**2.2. Analysis.** Mass density profiles across a membrane were computed for the porphyrin center of mass positions and for a number of different groups in the lipids. The profiles for the lipid groups were averaged over the whole time of the simulations. However, since 9 of the 12  $\text{Hp}^{2-}$  molecules were found to partition into the membrane after about 100 ns of the simulation, the density profiles for porphyrin were averaged over the last 100 ns of the trajectories.

The lateral diffusion coefficient,  $D_L$ , was computed by means of the Einstein's relation

$$D_L = \lim_{t \rightarrow \infty} \frac{\text{MSD}(t)}{2dt} \quad (1)$$

where  $d$  is the number of translational degrees of freedom (here  $d = 2$ ) and  $\text{MSD}(t)$  is the mean-squared displacement

$$\text{MSD}(t) = \langle |r(t + \tau) - r(\tau)|^2 \rangle \quad (2)$$

where  $r(t)$  is the position of the center of mass at time  $t$  and  $\langle \dots \rangle$  denotes averaging over different initial times during a simulation run and also over all the considered molecules in the system. The motion of molecules ( $\text{Hp}$ , lipids) was here computed for the center of mass of the given molecule, and it was considered with respect to the center of mass of the lipid monolayer in which the molecule resided.<sup>35</sup>

For rotational motion of porphyrin, we considered the rotational autocorrelation functions (RACFs) of the porphyrin ring plane:

$$C_l(\tau) = \langle P_l(n(t_0) \cdot n(t_0 + \tau)) \rangle_{t_0} \quad (3)$$

where  $P_l$  is the  $l$ th Legendre polynomial,  $n$  is a fixed unit vector in the molecule,  $t_0$  and  $\tau$  are the initial and lap times, respectively, and  $\langle \dots \rangle_{t_0}$  denotes an averaging over different initial times within a simulation run and over all molecules in the system. In this article, we considered the first Legendre polynomial  $P_1(\cos \theta) = \cos \theta$ . The rotational autocorrelation functions were assumed to decay in a monoexponential manner

$$C(t) = A_0 + A_1 e^{-t/\tau} \quad (4)$$

where  $t$  is time,  $\tau$  is correlation time, and  $A_0$  and  $A_1$  are amplitudes. The parameter  $A_0$  is often nonzero due to the fact that the rotation of the molecule is restricted in the direction of the bilayer normal. If the above exponential decay holds to a sufficient degree, it implies that the rotational diffusion coefficient (for the given rotation) can be assumed to follow the relation  $D_R \sim 1/\tau$ .

To estimate the number of hydrogen bonds, we used the same geometrical criteria as in the previous paper:<sup>36</sup> An H bond was assumed to be formed when the O–O distance was  $\leq 3.25$

$\text{\AA}$  and the angle between the O–O vector and the OH bond was  $\leq 35^\circ$ .

### 3. RESULTS

**3.1. Nonequilibrium Assembly of Hematoporphyrin Close to a Lipid Membrane.** We first characterized the self-assembly process of Hp molecules close to and in the membranes. Figure S1 (see the Supporting Information) depicts how Hp molecules move along the membrane normal direction (Z-coordinate); Figures S1a and S1b describe the motions of  $\text{Hp}^0$ , and Figures S1c, S1d, and S1e the movement of  $\text{Hp}^{2-}$ . In the plots, the interfaces of the bilayer–water and polar–hydrophobic regions are shown as solid and dashed gray lines, respectively, describing the average positions of the nitrogen atoms of the choline groups and the carbonyl groups of the acyl chains.

The neutral  $\text{Hp}^0$  molecules, which were initially inserted in the center of the bilayer migrated immediately to the interface between polar and hydrophobic membrane regions and remained there for the rest of the simulation time. In a similar manner, the molecules initially placed in the aqueous phase diffused to the same interface, the process taking no more than 50 ns. Over the last 100 ns of the simulations, the porphyrin rings of all  $\text{Hp}^0$  molecules occupied positions close to the POPC carbonyl groups, and did not display any tendency to move to the center of the lipid bilayer or to the aqueous phase.

The dianionic  $\text{Hp}^{2-}$  behaved similarly to a certain degree but with more preference to the water phase. In this case, the molecules initially placed in the center of the bilayer moved quickly (in less than 1 ns) away from the center to the polar region close to or above the carbonyl groups, and stayed there for the rest of the simulation. From the six  $\text{Hp}^{2-}$  anions placed initially in the aqueous phase, four molecules entered the membrane interfacial region while the remaining two stayed in the water phase. In most cases, the molecules entered the membrane within less than 50 ns, though in one case the event occurred also at the end of the simulation. After partitioning into the POPC bilayer, the dianions occupied a location within the polar region. The two molecules, which did not enter the lipid bilayer, formed a dimer which remained stable during the whole simulation. This suggests that the free energy barrier for entering the bilayer is larger for a dimer compared to a  $\text{Hp}^{2-}$  monomer.

In none of the cases discussed above did we find translocation of Hp across the membrane. Apparently, the barrier for translocation is rather large, though its determination would require free energy calculations that were not in the scope of this study and remain to be discussed elsewhere.

**3.2. Porphyrin Location.** Selected snapshots taken at the end of the simulations, illustrating the location and orientation of porphyrin in the POPC bilayer, are shown in Figure 2c and f. They indicate that, as the system has settled down after the self-assembly process of Hp, both  $\text{Hp}^0$  and  $\text{Hp}^{2-}$  prefer a location right below the water–membrane interface. To elucidate the position of the porphyrins with respect to the lipid molecules, we calculated their mass density profiles across the membrane.

Figure 3 depicts that both forms of porphyrin are more broadly distributed compared to any of the molecular groups in POPC studied here. Also, it turns out that the distribution of the anionic Hp is broader compared to that of the neutral form, and that  $\text{Hp}^{2-}$  has several maxima, highlighting its preference to both the membrane and the water phase.

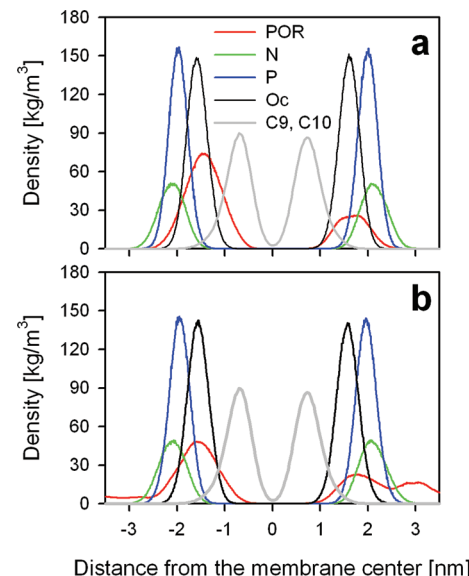


**Figure 3.** Mass density profiles of porphyrins and the selected POPC atoms along the bilayer normal as averaged over the last 100 ns of the trajectories and also over the simulated systems:  $\text{Hp}^0$  (a) and  $\text{Hp}^{2-}$  (b). The profiles are colored as follows: red lines, porphyrin rings; blue lines, phosphate groups; green lines, choline groups; black lines, carbonyl oxygens; and gray lines, double bonds.

$\text{Hp}^0$  is located preferentially slightly below the carbonyl group region (Figure 3a). Its profile has a maximum at  $\sim 1.5$  nm from the bilayer center and is partly overlapped by the profiles of both the choline and the phosphate groups as well as those of the double bonds of lipids. As for  $\text{Hp}^{2-}$ , Figure 3b shows that they occupy the region slightly above the carbonyl groups of the acyl chains. The mass density profile has a maximum at  $\sim 1.7$  nm and is, similarly to  $\text{Hp}^0$ , partly overlapped by the choline and the phosphate groups, and the profiles of lipid double bonds. The second maximum, appearing at  $\sim 3$  nm, indicates the above-mentioned tendency of  $\text{Hp}^{2-}$  to partially remain in the aqueous phase.

To check the effect of Hp molecules on the properties of the POPC bilayer, the order parameters ( $S_{\text{mol}}$ ) were calculated for pure and porphyrin-loaded membrane. Figure S2 (Supporting Information) presenting the values of  $S_{\text{mol}}$  shows that the ordering of lipid molecules was basically not affected at all. For both  $\text{Hp}^0$  and  $\text{Hp}^{2-}$ , at the low concentration used in the simulations, the effect of porphyrin was essentially marginal.

**3.3. Orientation of Porphyrin in a Membrane.** To describe the orientation of the porphyrin ring inside the membrane, we used two parameters: the angle  $\theta_r$  between the vector along the ring plane (see inset in Figure 4a) and the normal to the membrane and the angle  $\theta_n$  between the normal of the Hp ring and the bilayer normal.

The normalized distributions  $P(\theta_r)$  for all  $\text{Hp}^0$  and for  $\text{Hp}^{2-}$  molecules which entered the membrane are shown in Figure 4a. Both distributions are very broad with maxima at  $\sim 70^\circ$  for the neutral form and at  $\sim 45^\circ$  for the ionic form. To gain more quantitative data about the ring orientation, Gaussian functions were fitted to the distributions. In the case of  $\text{Hp}^0$ , an almost ideal fit was observed with two Gaussians of which the more dominant one with a maximum at  $69^\circ$  contributed to  $\sim 98\%$  of the molecules. A minor peak was also observed at  $\sim 27^\circ$ , contributing to the remaining 2%. In the case of  $\text{Hp}^{2-}$ , an excellent fit was again obtained with two Gaussians with

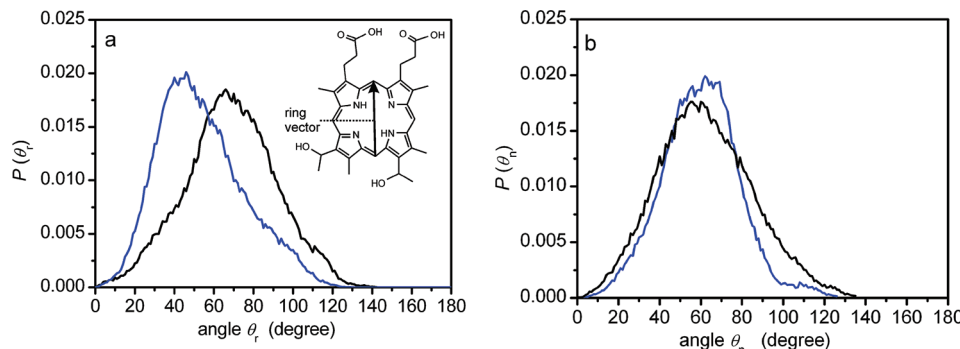


**Figure 4.** (a) Probability distributions,  $P(\theta_r)$ , of the angles  $\theta_r$  between the ring vector (shown in the inset) and bilayer normal for  $\text{Hp}^0$  (black line) and  $\text{Hp}^{2-}$  (blue line) over the last 100 ns of the trajectories. (b) Probability distributions,  $P(\theta_n)$ , of the angle  $\theta_n$  between the normal to the porphyrin ring and the bilayer normal over the last 100 ns of the trajectories for  $\text{Hp}^0$  (black line) and  $\text{Hp}^{2-}$  (blue line).

maxima at 42° (contributing to ~52% of the molecules) and 67°.

The data in Figure 4b show that the distributions of  $\theta_n$  for  $\text{Hp}^0$  and  $\text{Hp}^{2-}$  are largely similar. They are also broad, showing that the ring plane has a great orientational freedom. The distributions bring about that the vector normal to the ring plane makes an average angle of 60° with the bilayer normal. Therefore, a vector parallel to the plane of the porphyrin ring should make an average angle of 30° with the bilayer normal. Thus, the plane of the porphyrin ring aligns almost parallel to the lipid acyl chains, as is also highlighted by Figure 2c and f.

To get more insight into the arrangement of the porphyrin molecules inside the polar region of the POPC membrane, the density profiles of the oxygen atoms in the two 1-hydroxyethyl and carbonyl groups were calculated, as these are the most distant groups in the chemical structure of Hp. As shown in Figure 5, the hydroxyl groups are located deeper in the

hydroxyethyl group is attached to a different side of the porphyrin ring (see the Hp structure in Figure 1).

As can be expected from the results of the angle  $\theta_n$ , the arrangement of the  $\text{Hp}^{2-}$  molecules in the POPC bilayer is more complicated. Indeed, the distribution of the carboxylic oxygens is not symmetric and has a shoulder at the larger distance side from the membrane center. Two Gaussian distributions fitted (data not shown) to the data resulted in maxima at positions of  $1.88 \pm 0.23$  and  $2.30 \pm 0.34$  nm. These correspond well to the two different  $\theta_r$  angles of the  $\text{Hp}^{2-}$  molecule with respect to the membrane normal. The analysis of the profile of the hydroxyl groups revealed that at least three Gaussian functions were needed for a reasonable fit, which resulted in maxima at  $0.84 \pm 0.20$ ,  $1.57 \pm 0.29$ , and  $2.28 \pm 0.21$  nm.

**3.4. Dynamics.** We next dealt with the dynamic behavior of the porphyrin and the lipids inside the membrane. In particular, we focused on their lateral and rotational diffusion behavior, the emphasis being on porphyrin. The results of the mean-squared displacement (MSD) for lateral diffusion are shown in Figure 6.

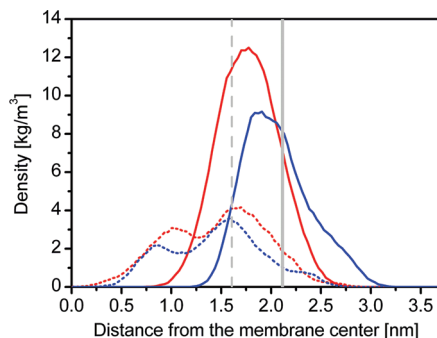


**Figure 5.** Symmetrized density profiles of the oxygen atoms in the two 1-hydroxyethyl groups (dotted lines) and the two carbonyl groups (solid lines) for  $\text{Hp}^0$  (red lines) and  $\text{Hp}^{2-}$  (blue lines). The center of mass positions of the nitrogen atoms of the choline (gray line) and the carbonyl groups of the POPC acyl chains (dashed gray lines) are also shown.

membrane than the more polar carboxyl groups, where the latter protrude into the headgroup region or even into the water phase.

In the case of the neutral form of porphyrin, the carboxylic oxygen atoms are symmetrically distributed around a maximum at  $1.76 \pm 0.32$  nm. Meanwhile, the distribution of the oxygens in 1-hydroxyethyls has two maxima, one at  $0.94 \pm 0.25$  nm and another at  $1.71 \pm 0.33$  nm (based on fitting of several overlapping Gaussian distributions (data not shown)). The two observed maxima in this profile result from the fact that each 1-

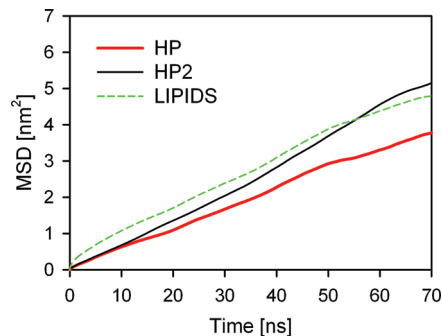


**Figure 6.** Mean square displacement (MSD) in the plane of the membrane, describing the lateral motion of  $\text{Hp}^0$  (red line),  $\text{H}^{2-}$  (black line), and POPC (dotted green line).

The lateral diffusion coefficients,  $D_L$ , turned out to be  $(1.35 \pm 0.06)$  and  $(1.90 \pm 0.05) \times 10^{-7}$  cm<sup>2</sup>/s for  $\text{Hp}^0$  and  $\text{Hp}^{2-}$ , respectively. For comparison, the lateral diffusion coefficient of lipids was found to be  $(1.68 \pm 0.04) \times 10^{-7}$  cm<sup>2</sup>/s. The lateral diffusion of both porphyrin forms is therefore comparable to that of POPC molecules. This should not be surprising, since porphyrin resides mainly in the densest region of the membrane where free volume is the smallest,<sup>37</sup> implying that the diffusion of porphyrin in the plane of the membrane occurs in a similar manner as the diffusion of the lipids.

Comparison of our diffusion results to experiments is difficult, since the  $D_L$  values of porphyrins in lipid membranes have not been reported previously in the literature. However, our data are in agreement with a mutual lateral diffusion coefficient of  $(1.8 \pm 0.1) \times 10^{-7} \text{ cm}^2 \text{ s}^{-1}$  obtained from fluorescence quenching of fluorazophore-L by  $\alpha$ -tocopherol at 300 K in POPC membrane.<sup>38</sup> The data for lipid diffusion is also in good agreement with experiments, since NMR studies of POPC diffusion have reported a lateral diffusion coefficient of  $1.4 \times 10^{-7} \text{ cm}^2/\text{s}$  at 308 K and  $1.9 \times 10^{-7} \text{ cm}^2/\text{s}$  at 313 K.<sup>39</sup>

To describe the rotational motion of the porphyrin molecule, we calculated the rotational autocorrelation functions (RACFs) for the vector perpendicular to the porphyrin ring plane and determined the characteristic correlation time associated with rotational motion, assuming eq 3 to hold to a reasonable degree. The RACF results together with fits to eq 4 are shown in Figure 7. They yield the rotational correlation times  $48 \pm 2$

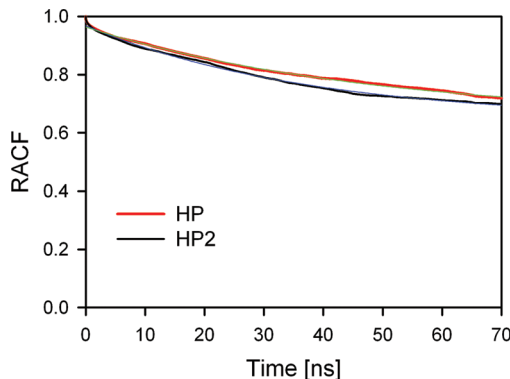


**Figure 7.** Rotational autocorrelation function (RACF) of the porphyrin ring of  $\text{Hp}^0$  (red line) and  $\text{Hp}^{2-}$  (black line). The solid thick lines describe the simulation data, and the thin lines are fits to eq 4.

and  $37 \pm 1$  ns for  $\text{Hp}^0$  and  $\text{Hp}^{2-}$ , respectively. The data suggest that the rotational dynamics of porphyrin is somewhat faster in the case of  $\text{Hp}^{2-}$  compared to the neutral porphyrin. This is in line with the previous observation that lateral diffusion of the dianionic porphyrin is faster compared to the neutral case, suggesting that the free volume around  $\text{Hp}^{2-}$  is larger than in the vicinity of  $\text{Hp}^0$ . Nonetheless, care should be taken in interpreting the data since the rotational correlation function clearly decays slowly compared to the simulation time scale. For a more accurate description, the simulation time scale should be extended by at least 1–2 orders of magnitude, but unfortunately, that is not feasible in the present case.

**Table 1. Number of Hydrogen Bonds (H-Bonds) between the Porphyrin Carboxyl ( $\text{Hp}-\text{Oc}$ ) or 1-Hydroxyethyl ( $\text{Hp}-\text{OH}$ ) Groups with POPC or Water<sup>a</sup>**

	$\text{Hp}^0$	$\text{Hp}^{2-}$
number of H-bonds $\text{Hp}-\text{OH}\cdots\text{POPC}$	0.88	0.63
number of H-bonds $\text{Hp}-\text{COOH}\cdots\text{POPC}$	1.32	1.38
number of H-bonds $\text{Hp}-\text{OH}\cdots\text{OH}_2$	1.52	2.31
number of H-bonds $\text{Hp}-\text{Oc}\cdots\text{H}-\text{OH}$ or $\text{Hp}-\text{COOH}\cdots\text{OH}_2$	2.69	7.21
number of charge pairs $\text{HpOc}-\text{N}^+(\text{CH}_3)_3$	2.69	1.88
number of charge pairs $\text{HpOH}-\text{N}^+(\text{CH}_3)_3$	5.57	0.33

<sup>a</sup>Numbers of charge pairs between the porphyrin oxygens and the lipid choline groups ( $\text{N}^+(\text{CH}_3)_3$ ). The results are given per one porphyrin molecule.

**3.5. Porphyrin–POPC and Porphyrin–Water Interactions.** Porphyrin is located in that part of a bilayer, which interacts with water and contains polar groups. Therefore, it is quite plausible that hydrogen bonds (H-bonds) would form between porphyrin and POPC and between porphyrin and water. In the case of the porphyrin–POPC pair, H-bonds can be formed between (i) one of the 1-hydroxyethyl groups of  $\text{Hp}^0$  or  $\text{Hp}^{2-}$  and nonester oxygen in the phosphate group of POPC ( $\text{Hp}-\text{OH}\cdots\text{POPC}$ ) and (ii) the carboxylic OH group of  $\text{Hp}^0$  and the nonester oxygen of the phosphate group of POPC ( $\text{Hp}-\text{COOH}\cdots\text{POPC}$ ). In the case of porphyrin–water pairs, hydrogen bonds can be formed between (iii) one of the 1-hydroxyethyl groups of  $\text{Hp}^0$  or  $\text{Hp}^{2-}$  and an oxygen atom of a water molecule ( $\text{Hp}-\text{OH}\cdots\text{OH}_2$ ) and (iv) the carbonyl oxygen of  $\text{Hp}^0$  or  $\text{Hp}^{2-}$  and an OH group of a water molecule ( $\text{Hp}-\text{Oc}\cdots\text{H}-\text{OH}$ ) or a carboxylic OH group of  $\text{Hp}^0$  and an oxygen atom of a water molecule ( $\text{Hp}-\text{COOH}\cdots\text{OH}_2$ ). The calculated numbers of hydrogen bonds are given in Table 1.

We also considered the existence of charge pairs between the porphyrin oxygen atoms both in the 1-hydroxyethyl and carboxylic groups and the positively charged choline groups.<sup>36</sup> Numbers of these interactions are given in Table 1. The number of polar interactions between porphyrin molecules and lipids is found to be substantial. In the case of  $\text{Hp}^{2-}$ , more interactions with water were observed but at the expense of interactions with the choline groups of POPC.

**3.6. Porphyrin–Porphyrin Interactions.** As mentioned earlier in this article, we observed the formation of a stable dimer of  $\text{Hp}^{2-}$  in the water phase; for a snapshot, see Figure 8.

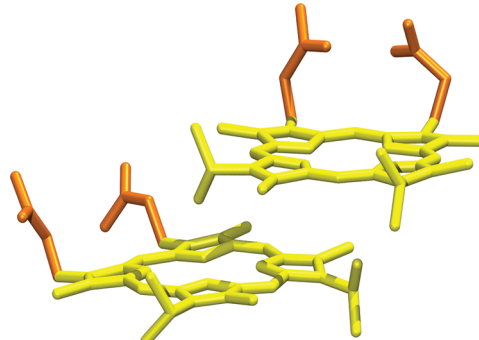


**Figure 8.** Snapshot of the  $\text{Hp}^{2-}$  dimer in the aqueous phase.

It seems that the lifetime of that dimer is longer than the simulation time (200 ns), since the species formed at the beginning of the simulation remained stable until the end of the simulation run. The average distance between the porphyrin rings in the dimer was  $0.426 \pm 0.015$  nm. The angle between

the ring vectors (see Figure 5a) was found to be  $160 \pm 30^\circ$ . In the case of the molecules which entered the membrane, we also observed formation of a dimer; however, in this case, the lifetime was much shorter,  $\sim 30$  ns. Therefore, we assumed that the formation of porphyrin dimers inside a membrane is possible, but these species are much less stable compared to those in the aqueous environment.

#### 4. DISCUSSION

Hematoporphyrin belongs to a group of so-called dicarboxylic porphyrins. This is due to its chemical structure, which consists of the tetrapyrrole ring with two propionic acids attached at the same side of the ring at positions six and seven. Such a structure causes these compounds to be amphiphilic. In the previous studies on the acid–base properties of Hp, the ionization constants of the acid groups ( $pK_a$ ) were determined. Brault et al. determined the two  $pK_a$  values to be 5.0 and 5.4.<sup>40</sup> Barret et al. reported slightly different values of 6.0 and 6.8.<sup>41</sup> Furthermore, the ionization constants for the two carboxylate groups of the zinc complex of Hp (ZnHp) were determined to be  $5.7 \pm 0.1$  and  $6.9 \pm 0.05$ .<sup>10</sup> On the basis of these values, one can easily conclude that at the physiological pH of 7.4 more than 76% of Hp molecules are deprotonated at both propionic acid groups. For this reason, in this study, we have simulated systems that contained two forms of Hp, namely, the neutral and dianionic ones in a POPC membrane that was used as a model of the mammalian cellular membrane.

There are several experimental pieces of evidence confirming that Hp can interact with a lipid bilayer.<sup>8,10,42</sup> The previous studies have shown that porphyrins ionized at their imino nitrogens do not incorporate into membranes, while deprotonation of the carboxylic moieties does not prevent their partitioning but rather places them close to the water–lipid interface.<sup>10,38</sup> In studies of ZnHp binding to liposomes, one has observed a significant effect of pH on the so-called binding constant ( $K_b$ ) to liposomes.<sup>10</sup>  $K_b$  is an experimentally determined parameter, which indicates the affinity of a given compound to partition into a lipid membrane. It was shown that an increase in pH from 5.4 (the neutral form of ZnHp) to 9.0 (the dianionic form of ZnHp) caused a 3.9-fold decrease in the value of  $K_b$ . The partitioning of free Hp to the lipid phase was also found to be strongly dependent on the acidity of the bathing solution.<sup>42</sup> Thus, the ionized porphyrin shows a much lower affinity to incorporate itself into a lipid membrane. However, the preferred location of Hp inside a lipid bilayer has not been recognized in experimental studies.

Our simulation results are in line with experimental findings. As we have shown, both forms of Hp are able to partition into the POPC membrane.  $\text{Hp}^{2-}$  was found to exhibit a lower affinity to the bilayer, since two of the six cases (regarding molecules initially placed in the aqueous phase in three different simulations) stayed in this environment for the whole simulation period. Moreover, our studies allowed us to determine the preferred location of the  $\text{Hp}^0$  and  $\text{Hp}^{2-}$  in the membrane.

Usually, by specifying the position of a molecule in a membrane, the location of its center of mass is determined. We found that the mass centers of  $\text{Hp}^0$  and  $\text{Hp}^{2-}$  are about 1.5 and 1.7 nm, respectively, from the center of the POPC membrane. However, one should be aware of the thickness of the POPC bilayer and the dimensions of the Hp molecule. Lipid membranes are highly dynamic structures, and the lipid positions therefore highly fluctuate due to thermal noise.<sup>43</sup>

This is the reason why the position of each fragment of the lipids projected onto the bilayer normal, and averaged over time, is Gaussian distributed, as shown in Figure 3. Similar Gaussian distributions of the fragment positions were determined experimentally for 1,2-dioleoyl-sn-glycero-3-phosphatidylcholine (DOPC) using the joint refinement of X-ray and neutron diffraction data.<sup>39</sup> Therefore, there is no firm definition of the bilayer thickness. However, it is reasonable to assume this parameter as an average N–N spacing (the distance between average positions of nitrogen atoms in two leaflets of the bilayer). We calculated the POPC membrane thickness as  $4.2 \pm 0.2$  nm. That parameter was determined experimentally for the DOPC bilayer to be  $4.36 \pm 0.04$  nm,<sup>39</sup> which is very close to our value. Since the internal structure of a membrane is heterogeneous, it has been proposed to divide the POPC bilayer into four regions along the membrane normal direction:<sup>14,44</sup> (i) region I of the lowest density contains almost exclusively the lipid tails (about 0–1.0 nm from the bilayer center); (ii) region II contains a diverse mixture of functional groups, mostly the carbonyl groups and a portion of the headgroups, and is effectively the interface between the hydrocarbon chain region and the polar region (1.0–1.8 nm from the center of the bilayer); (iii) region III contains the bulk of the headgroups and a substantial amount of water (1.8–2.5 nm from the center of the bilayer); and (iv) region IV consists mostly of bulk water, with small amounts of the headgroups (>2.5 nm from the membrane center). In this description, the thickness of one leaflet of the POPC membrane is about 2.5 nm (see Figure S1 in the Supporting Information of ref 40). The length of the Hp molecule based on its optimized structure was found to be  $\sim 1.5$  nm, as measured between the carbon atom of the methyl in the 1-hydroxyethyl group and the oxygen atom in the carboxyl group on the same side of the porphyrin ring. Concluding, Hp is a relatively large molecule compared to the POPC bilayer dimensions and its location in the membrane is spread over the different membrane regions.

The appearance of the negative charges at the carboxylic groups had little effect on the depth of the porphyrin ring in the membrane. The maximum of the mass density profile shifts only about 0.2 nm toward the surface of the POPC bilayer. However, deprotonation of the carboxylic groups was found to have a very pronounced effect on the orientation of the porphyrin ring. The orientation of  $\text{Hp}^0$  and  $\text{Hp}^{2-}$  inside the POPC membrane should be analyzed in comparison to the arrangement of the acyl chains of lipid molecules. The average tilt angle of the palmitoyl groups was calculated from the cosine of the angle between the bilayer normal and the average vector linking the carbon atom at the end of the palmitoyl chain and the carbonyl carbon atom of the same chain. By doing so, the average tilt angle of the palmitoyl chains in the POPC bilayer was observed to be  $\sim 31^\circ$ . Moving on, we used two parameters to determine the orientation of the Hp molecule inside the POPC membrane. The first one was the vector that is normal to the porphine ring of Hp. This vector made an average angle of  $\sim 30^\circ$  with the bilayer normal for both forms of the porphyrin, indicating that the ring plane preferentially adopts an orientation where it is aligned with the lipid acyl chains. Second, since the Hp molecule is asymmetric, we have additionally used another parameter to describe the orientation of Hp, using the ring vector inscribed in the Hp ring and pointing to the side at which the two propionic acid groups were attached (see Figure 5). The distributions of  $\theta_r$  for both forms of the Hp molecule were found to be completely

different. In the case of Hp<sup>0</sup>, the ring vector made an average angle of ~70° with the bilayer normal, indicating that Hp<sup>0</sup> molecules are arranged in a bilayer in such a way that the propionic acid groups are almost parallel to the POPC membrane surface (Figure 2c). This arrangement is likely due to strong interactions of the Hp polar groups (two carboxylic and hydroxylic) with lipid polar groups, as shown in Table 1. In the case of Hp dianions, those interactions were attenuated by formation of a large number of H-bonds between Hp-Oc groups and water molecules. In this case, the distribution of  $\theta_r$  had a maximum at about 40°, meaning that the dianions were arranged with their long axis almost parallel to the acyl chains of lipid molecules, and with the carboxylic groups being in region III or partially in region IV of the POPC membrane.

Unfortunately, most porphyrins, native and synthetic, are not sufficiently soluble in aqueous solution, particularly near neutral pH, to allow for extensive examination of their physicochemical properties. Two processes of porphyrins in heterogeneous systems containing aqueous and membrane phases have been studied with hematoporphyrin: dimerization equilibrium in the aqueous phase and porphyrin–membrane binding equilibrium using liposomes as models for biological membranes.<sup>45</sup> The relationship of aqueous aggregations and membrane binding was probed, and the porphyrin aggregation state in the membrane was also assessed. The dimerization equilibrium constant, at neutral pH and 310 K, was found to be  $2.8 \times 10^5$  M<sup>-1</sup> for Hp. Over a porphyrin concentration range extending from the monomer-dominated to dimer-dominated systems, it was found that only monomers are bound to the membrane. The respective monomer–liposome binding constants were found to be independent of the initial monomer/dimer distribution in the aqueous phase. The monomer–liposome interaction was observed to perturb the initial monomer/dimer distribution in the aqueous phase, so that the monomers residing under equilibrium conditions in the membrane originate from both monomers and dimers in the aqueous phase. Importantly, formation of a porphyrin dimer in the aqueous phase was confirmed in our simulations, too.

## 5. CONCLUSIONS

We used computer simulations to investigate the behavior of neutral and charged forms of Hp, a dipropionic porphyrin, in the presence of a zwitterionic bilayer that was used as a model for the mammalian cellular membrane. Our simulations provide one with insight on the localization, orientation, and dynamics of Hp inside the lipid bilayer. In agreement with experiments, we found that both forms of Hp partition into the membrane, but dications have a lower affinity for the membrane environment compared to the neutral form. The center of mass of the porphyrin molecule was found to localize preferentially in the lipid carbonyl region of the membrane. However, as Hp molecules are relatively large compared to the thickness of the membrane, their density distribution covers several different regions inside a membrane, with 1-hydroxyethyl groups buried in the most hydrophobic part of the membrane (region I) and the carboxylic groups being near or in the lipid headgroup region (regions II or III), or even in the aqueous phase (region IV) in the case when these groups are dissociated. Such localization of the dye results from strong interactions between the polar groups of the porphyrin and the lipids and water. Our results are useful for understanding of cellular up-take of porphyrin-based photosensitizers and for designing of new photosensitizers for PD and PDT.

## ■ ASSOCIATED CONTENT

### ■ Supporting Information

Gromacs topology file of a porphyrin molecule with corresponding structure file. The topology file includes partial charges. Additional figures showing trajectories of center of mass of Hp molecules along the bilayer normal (Figure S1) and a profile of the molecular order parameter (Figure S2) are also provided. This material is available free of charge via the Internet at <http://pubs.acs.org>.

## ■ AUTHOR INFORMATION

### Corresponding Author

\*Phone: +48 12 6632020 (M.K.); +358 40 198 1010 (T.R.). Fax: +48 12 6340515 (M.K.); +358 3 3115 3015 (T.R.). E-mail: kepczyns@chemia.uj.edu.pl (M.K.); tomasz.rog@gmail.com (T.R.).

### Notes

The authors declare no competing financial interest.

## ■ ACKNOWLEDGMENTS

This project was operated within the Foundation for Polish Science Team Programme cofinanced by the EU European Regional Development Fund, PolyMed, TEAM/2008-2/6. T.R. and I.V. wish to thank the Academy of Finland for financial support. M.K. acknowledges the Polish Ministry of Science and Higher Education for financial support in the form of Grant No. N N209 118937. For computational resources, we wish to thank the Finnish IT Centre for Scientific Computing. M.S. thanks the National Doctoral Programme in Informational and Structural Biology for financial support.

## ■ REFERENCES

- (1) Dougherty, T. J.; Kaufman, J. E.; Goldfarb, A.; Weishaupt, K. R.; Boyle, D.; Mittelman, A. *Cancer Res.* **1978**, *38*, 2628–2635.
- (2) Dougherty, T. J.; Gomer, C. J.; Henderson, B. W.; Jori, G.; Kessel, D.; Korbelik, M.; Moan, J.; Peng, Q. *J. Natl. Cancer Inst.* **1998**, *90*, 889–905.
- (3) Jori, G.; Reddi, E.; Cozzani, I.; Tomio, L. *Br. J. Cancer* **1986**, *53*, 615–621.
- (4) Jori, G.; Beltramini, M.; Reddi, E.; Salvato, B.; Pagnan, A.; Ziron, L.; Tomio, L.; Tsanov, T. *Cancer Lett.* **1984**, *24*, 291–297.
- (5) Lipson, R. L.; Blades, E. J.; Olsen, A. M. *J. Natl. Cancer Inst.* **1961**, *26*, 1–11.
- (6) Dougherty, T. J.; Grindey, G. B.; Weishaupt, K. R.; Boyle, D. J. *Natl. Cancer Inst.* **1975**, *55*, 115–121.
- (7) Gupta, S.; Dwarakanath, B. S.; Muralidhar, K.; Jain, V. *J. Photochem. Photobiol. B* **2003**, *69*, 107–120.
- (8) Aharon, D.; Weitman, H.; Ehrenberg, B. *Biochim. Biophys. Acta* **2011**, *1808*, 2031–2035.
- (9) Kepczynski, M.; Pandian, R. P.; Smith, K. M.; Ehrenberg, B. *Photochem. Photobiol.* **2002**, *76*, 127–134.
- (10) Kepczynski, M.; Ehrenberg, B. *Photochem. Photobiol.* **2002**, *76*, 486–492.
- (11) Kuzelova, K.; Brault, D. *Biochemistry* **1995**, *34*, 11245–11255.
- (12) Ricchelli, F.; Gobbo, S. *J. Photochem. Photobiol. B* **1995**, *29*, 65–70.
- (13) Bronstein, I.; Afri, M.; Weitman, H.; Frimer, A. A.; Smith, K. M.; Ehrenberg, B. *Biophys. J.* **2004**, *87*, 1155–1164.
- (14) MacCallum, J. L.; Tielemans, D. P. *Curr. Top. Membr. Transp.* **2008**, *60*, 227–256.
- (15) Xiang, T.-X.; Anderson, B. D. *Adv. Drug Delivery Rev.* **2006**, *58*, 1357–1378.
- (16) Curdova, J.; Caplova, P.; Plasek, J.; Repakova, J.; Vattulainen, I. *J. Phys. Chem. B* **2007**, *111*, 3640–3650.

- (17) Stepniewski, M.; Bunker, A.; Pasenkiewicz-Gierula, M.; Karttunen, M.; Rög, T. *J. Phys. Chem. B* **2010**, *114*, 11784–11792.
- (18) Jorgensen, W. L.; Maxwell, D. S.; Tirado-Rives, J. *J. Am. Chem. Soc.* **1996**, *118*, 11225–11236.
- (19) Takaoka, Y.; Pasenkiewicz-Gierula, M.; Miyagawa, H.; Kitamura, K.; Tamura, Y.; Kusumi, A. *Biophys. J.* **2000**, *79*, 3118–3138.
- (20) Bayly, C. I.; Cieplak, P.; Cornell, W.; Kollman, P. A. *J. Phys. Chem.* **1993**, *97*, 10269–10280.
- (21) Cornell, W. D.; Cieplak, P.; Bayly, C. I.; Kollmann, P. A. *J. Am. Chem. Soc.* **1993**, *115*, 9620–9631.
- (22) Franci, M. M.; Chirlian, L. E. *Rev. Comput. Chem.* **2000**, *14*, 1–31.
- (23) Singh, U. C.; Kollman, P. A. *J. Comput. Chem.* **1984**, *5*, 129–45.
- (24) Besler, B. H.; Merz, K. M., Jr.; Kollman, P. A. *J. Comput. Chem.* **1990**, *11*, 431–439.
- (25) Frisch, M. J.; Trucks, G. W.; Schlegel, H. B.; Scuseria, G. E.; Robb, M. A.; Cheeseman, J. R.; Montgomery, J. A., Jr.; Vreven, T.; Kudin, K. N.; Burant, J. C.; et al. *Gaussian 03*, revision C.02; Gaussian, Inc.: Wallingford, CT, 2004.
- (26) Jorgensen, W. L.; Chandrasekhar, J.; Madura, J. D.; Impey, R. W.; Klein, M. L. *J. Chem. Phys.* **1983**, *79*, 926–935.
- (27) Rög, T.; Martinez-Seara, H.; Munck, N.; Oresic, M.; Karttunen, M.; Vattulainen, I. *J. Phys. Chem. B* **2009**, *113*, 3413–3422.
- (28) Hess, B.; Bekker, H.; Berendsen, H. J. C.; Fraaije, J. G. E. M. *J. Comput. Chem.* **1997**, *18*, 1463–1472.
- (29) Parrinello, M.; Rahman, A. *J. Appl. Phys.* **1981**, *52*, 7182–7190.
- (30) Nose, S. *J. Chem. Phys.* **1984**, *81*, 511–519.
- (31) Essman, U.; Perera, L.; Berkowitz, M. L.; Darden, H. L. T.; Pedersen, L. G. *J. Chem. Phys.* **1995**, *103*, 8577–8592.
- (32) Rög, T.; Bunker, A.; Vattulainen, I.; Karttunen, M. *J. Phys. Chem. B* **2007**, *111*, 10146–10154.
- (33) Sepniewski, M.; Pasenkiewicz-Gierula, M.; Rog, T.; Danne, R.; Orlowski, A.; Karttunen, M.; Urtti, A.; Yliperttula, M.; Vuorimaa, E.; Bunker, A. *Langmuir* **2011**, *27*, 7788–7798.
- (34) Hess, B.; Kutzner, C.; van der Spoel, D.; Lindahl, E. *J. Chem. Theory Comput.* **2008**, *4*, 435–447.
- (35) Patra, M.; Karttunen, M.; Hyvönen, M. T.; Falck, E.; Lindqvist, P.; Vattulainen, I. *Biophys. J.* **2003**, *84*, 3636–3645.
- (36) Murzyn, K.; Rög, T.; Jezierski, G.; Kitamura, K.; Pasenkiewicz-Gierula, M. *Biophys. J.* **2001**, *81*, 170–183.
- (37) Falck, E.; Patra, M.; Karttunen, M.; Hyvönen, M. T.; Vattulainen, I. *Biophys. J.* **2004**, *87*, 1076–1091.
- (38) Gramlich, G.; Zhang, J.; Nau, W. M. *J. Am. Chem. Soc.* **2004**, *126*, 5482–5492.
- (39) Filippov, A.; Oradd, G.; Lindblom, G. *Biophys. J.* **2003**, *84*, 3079–3086.
- (40) Brault, D.; Vever-Bizet, C.; Le Doan, T. *Biochim. Biophys. Acta* **1986**, *857*, 238–250.
- (41) Barrett, A. J.; Kennedy, J. C.; Jones, R. A.; Nadeau, P.; Pottier, R. *H. J. Photochem. Photobiol., B* **1990**, *6*, 309–323.
- (42) Brault, D. *J. Photochem. Photobiol., B* **1990**, *6*, 79–86.
- (43) Wiener, M. C.; White, S. H. *Biophys. J.* **1992**, *61*, 434–447.
- (44) Kepczynski, M.; Kumorek, M.; Stepniewski, M.; Rög, T.; Kozik, B.; Jamróz, D.; Bednar, J.; Nowakowska, M. *J. Phys. Chem. B* **2010**, *114*, 15483–15494.
- (45) Margalita, R.; Cohen, S. *Biochim. Biophys. Acta* **1983**, *736*, 163–170.